Chemistry & Biology 13, 539–548, May 2006 DOI 10.1016/j.chembiol.2006.04.004

Targeting Retroviral Zn Finger-DNA Interactions: A Small-Molecule Approach Using the Electrophilic Nature of *trans*-Platinum-Nucleobase Compounds

Atilio I. Anzellotti,[1] Qin Liu,[1] Marieke J. Bloemink,[1] J. Neel Scarsdale,[2,3] and Nicholas Farrell[1,*]
[1]Department of Chemistry
Virginia Commonwealth University
PO Box 842006
Richmond, Virginia 23284
[2]Institute for Structural Biology & Drug Discovery
PO Box 980133
[3]Department of Biochemistry
PO Box 980614
Virginia Commonwealth University
Richmond, Virginia 23298

Summary

Noncovalent interactions are ubiquitous in ternary systems involving metal ions, DNA/RNA, and proteins and represent a structural motif for design of selective inhibitors of biological function. This contribution shows that small molecules containing platinated purine nucleobases mimic the natural DNA(RNA)-tryptophan recognition interaction of zinc finger peptides, specifically the C-terminal finger of HIV NCp7 protein. Interaction with platinum results in Zn ejection from the peptide accompanied by loss of tertiary structure. Targeting the NCp7-DNA interaction for drug design represents a conceptual advance over electrophiles designed for chemical attack on the zinc finger alone. These results demonstrate examples of a new platinum structural class targeting specific biological processes, distinct from the bifunctional DNA-DNA binding of cytotoxic agents like cisplatin. The results confirm the validity of a chemical biological approach for metallodrug design for selective ternary DNA(RNA)-protein interactions.

Introduction

The nucleocapsid NCp7 protein is an attractive target for antiviral drug design. Retroviral nucleocapsid proteins (NCps) from all strains of known retroviruses contain one or more copies of the conserved CCHC zinc finger or "knuckle" sequence Cys-X_2-Cys-X_4-His-X_4-Cys (X = variable) [1]. The nucleocapsid protein NCp7 of human immunodeficiency virus type I (HIV-I) contains two of these highly conserved zinc finger domains that are necessary for viral replication [2, 3]. NCps contribute to multiple steps of the viral life cycle, all of which seem to involve binding to single-stranded nucleic acids [4, 5]. NCp7 is known to have a high affinity for single-stranded nucleic acids [6] and has been shown to be a potent chaperone for general nucleic acid folding and unfolding [7]. The protein is required for correct encapsidation and packaging of viral RNA [8, 9], and in the virion, NCp7 is thought to stabilize the dimeric RNA genome through formation of a ribonucleoprotein complex [10].

*Correspondence: npfarrell@vcu.edu

Studies in vitro show that NCp7 can activate the retroviral RNA dimerization and also enhances the annealing of the $tRNA_3^{Lys}$ primer to the initiation site of reverse transcription, suggesting that correct genomic RNA packaging and reverse transcription depend upon NCp7 [11, 12]. The participation of the nucleocapsid protein in multiple steps in the virus life cycle and the relative rarity of the CCHC motif in cellular proteins make NCp7 an attractive target for antiviral drug design. Such an approach would be complementary to drugs such as protease inhibitors and nucleoside analogs aimed at other targets of the viral life cycle. Zinc fingers are estimated to represent 1% of the human genome—a total of 4500 C_2H_2 zinc finger domains from 564 proteins are recognized, whereas only 17 domains from nine proteins contain the CCHC zinc knuckle motif [13, 14].

The molecular details of the interaction of the entire HIV nucleocapsid protein NCp7 (See Figure 1) bound to the 20 bp SL3 Ψ-RNA recognition element have been elucidated by NMR spectroscopy [15]. The structure showed interactions between the guanine bases of the single-stranded G_6-G_7-A_8-G_9 tetraloop involving stacking and H-bonding interactions of the exposed G_7 and G_9 residues with Phe and Trp, respectively [15]. The complex formed between the (12–53) NCp7 fragment, encompassing the two Zn knuckles and the short linking region, and d(ACGCC), a single-stranded deoxynucleotide sequence corresponding to the shortest NCp7 binding site, showed similar features [16]. The indole ring of the W37 tryptophan residue is inserted between adjacent C and G bases and stacked on the latter [16]. An important recognition motif in both structures is thus the presence of guanine/tryptophan (and/or phenylalanine) stacking interactions. The presence of the W37 residue has been revealed as a key feature for molecular recognition from the zinc finger toward oligonucleotides, as surface plasmon resonance and other experiments have confirmed [17, 18]. The noncovalent interaction is conserved even for the more complex SL2 and SL3 domains in the Ψ-recognition element of the viral genome [15, 19].

In terms of drug development, covalent modification of the nucleocapsid protein has been achieved by use of electrophiles [20]. The electrophiles covalently modify the zinc binding site through cysteine oxidation or alkylation to thioether, resulting in eventual cleavage of the Zn-S bond and zinc ejection. Loss of tertiary structure and nucleic acid binding ability leads to inhibition of function and prevention of infectivity. An inherent challenge for all small-molecule electrophiles is selectivity. Some anti-HIV agents have been described that target the NCp7 protein without affecting cellular zinc finger proteins [21]. In general, there is little intrinsic selectivity in anti-HIV, Zn-ejecting drugs. Thus, a worthwhile approach is to search for antagonists of the RNA(DNA)-protein interaction [22]. In this latter respect, the recognition motif of guanine/tryptophan stacking is worthy of exploitation in design of NCp7 selective agents. Small molecules containing dual properties of protein-DNA recognition as well as zinc ejection capacity would

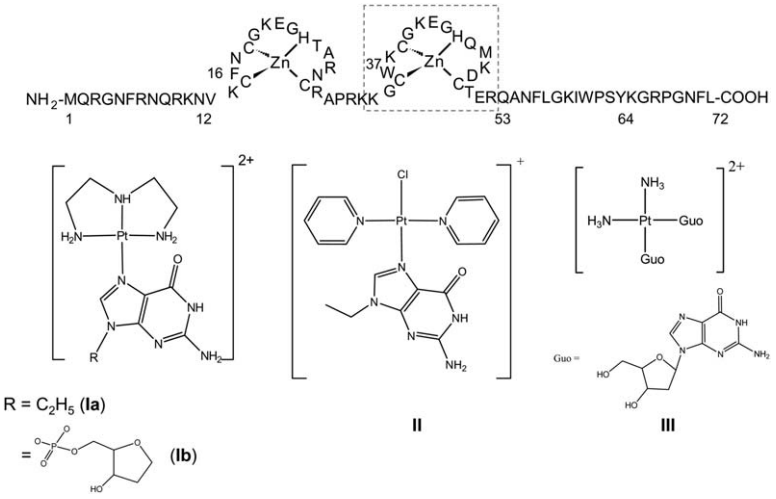

Figure 1. Top, Structure of the Entire HIV Nucleocapsid Protein and Bottom, Platinum Compounds Used in This Study

Ia, diethylenetriamine(9-ethylguanine)platinum(II). **Ib**, diethylenetriamine(guanosine)-platinum(II). **II**, *trans*-chlorobispyridine(9-ethylguanine)platinum(II). **III**, *cis*-diammine-bis(guanosine)platinum(II).

represent a building block for more selective interaction and therapeutic intervention.

Recently, we have proposed analogies between platinum and alkylating electrophiles and possible biological implications thereof. Fluorescence quenching experiments showed that the stacking interaction between nucleic acid bases and l-tryptophan is significantly enhanced upon nucleobase coordination to a Pt(II) center in $[Pt(dien)(L)]^{2+}$ (where L = 9-Ethylguanine (9-EtGH), 1-Methylcytosine (1-MeCyt), or their nucleotide monophosphate analogs 5′-GMP and 5′-CMP) [23, 24]. In the absence of a reactive leaving group, only noncovalent hydrogen-bonding and stacking interactions need to be taken into account. The effect mimics the enhancement of π-π stacking interactions to l-tryptophan upon methylation of purine and pyrimidine nucleic acid bases, attributable to a lowering in energy for the π-acceptor LUMO in the methylated nucleobase, thus improving the acceptor properties toward the π-donor HOMO of the amino acid [25]. In parallel studies, the interaction of *trans*-$[PtCl(9\text{-}EtGH)(py)_2]^+$ and the model zinc chelate $[Zn(bme\text{-}dach)]_2$ results in Zn ejection and eventual incorporation of Pt into the macrocycle [26]. Intermediate heterodinuclear thiolate bridged Pt-S-Zn species are formed. The thiolate ligand binding sites of $[Zn(bme\text{-}dach)]_2$ present a precedent for S-alkylation reactions in nature, being sufficiently nucleophilic to be readily alkylated [27].

We therefore wished to extend these findings to a biologically relevant system. This paper reports on model studies for recognition and fixation of platinum-nucleobase complexes on the C-terminal peptide (F2) of the HIV-NCp7 zinc knuckle. Figure 1 shows the structure of the nucleocapsid protein and the platinum compounds studied. The C-terminal peptide was chosen as proof of principle for a number of reasons: the knuckle contains the tryptophan moiety, and many observations indicate that the C-terminal Zn site is more reactive than the N-terminal sequence. The chemical composition of a zinc finger core as well as the local protein environment determine the reactivity of the zinc finger. Analysis through protein packing and electrostatic screening of 207 zinc fingers indicated that the C-terminal finger was one of the most reactive sites [28]. Experimentally, Cys^{49} is the most reactive cysteine, and theoretically, S^{49} is predicted to be the most nucleophilic site [28]. The complexes chosen for extensive study were $[Pt(dien)(9\text{-}EtGH)]^{2+}$ (**Ia**), $[Pt(dien)(5'\text{-}GMP)]$ (**Ib**), and *cis*-$[Pt(NH_3)_2(Guanosine)_2]^{2+}$ (**III**) capable of only noncovalent interactions and in addition, the *trans*-$[PtCl(9\text{-}EtGH)(py)_2]^+$ (**II**), containing one substitution-labile Pt-Cl bond suitable for covalent interactions. This paper shows that modulation of the $[PtCl(L)(L')(Nucleobase)]^+$ (L = NH_3, L′ = py, quin, etc., or L = L′ = py, etc.) structural motif is a viable approach to more effective and selective inhibitors of the zinc-finger-nucleic acid interaction and subsequent zinc ejection. Circular dichroism, fluorescence quenching, and electrospray ionization mass spectrometry (ESI-MS) were used to examine both noncovalent and covalent interaction of the platinum electrophiles with the 18-residue sequence corresponding to the C-terminal finger of HIV-NCp7. 1D and 2D NMR studies were used to confirm the nature of the interaction between the peptide and a model oligonucleotide d(TACGCC).

Results

The Zinc Finger-DNA Interaction

The formation of the zinc finger can be monitored by circular dichroism, ESI-mass spectrometry, and ^{1}HNMR spectroscopy (Figure 2). The mass spectrum shows peaks corresponding to the 2+ to 5+ states of the metallopeptide at m/z = 1144.1, 763.1, 572.8, and 458.6 amu, respectively (Figure 2A). The CD spectrum confirms the metallation with a red shift of the ellipticity minimum, typical of zinc-peptide formation (Figure 2B) [29–31]. The ^{1}H NMR spectrum in D_2O of the F2 zinc finger shows a downfield shift of the histidine protons and sharp signals at room temperature, indicating a conformationally stable structure (Figure 2C). Previous reports on the C-terminal domain had given spectra indicative of conformational lability [32]. The reasons for the discrepancy are unclear. The interactions of the 18-residue sequence corresponding to the N-terminal sequence of HIV-NCp7 with oligonucleotides d(ACGCC) and d(TTTGGTTT) have been studied by NMR methods [33, 34]. In the former case, the affinity is significantly less than for the intact finger [16]. The complementary study of the C-terminal F2 alone with a suitable oligonucleotide has not been

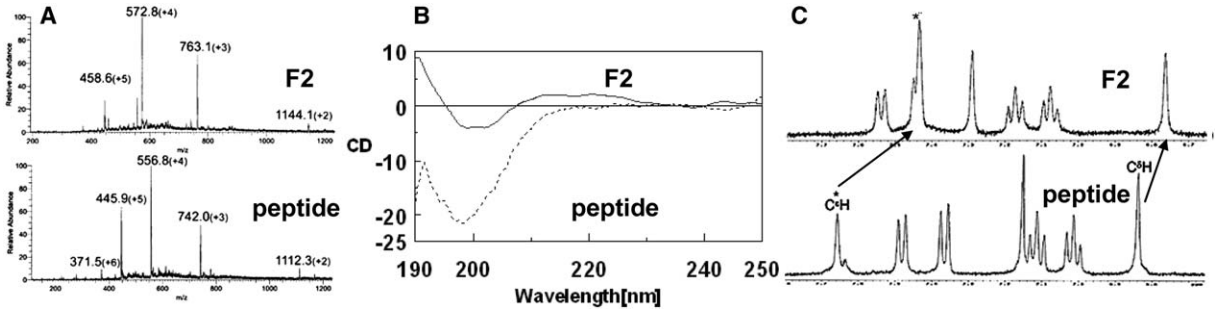

Figure 2. Spectroscopic Characterization of F2

Formation of the F2 exhibits changes that can be monitored by ESI-MS (A), circular dichroism (B), and ^{1}H-NMR (C) for the free peptide (bottom) upon coordination to Zn^{2+}. The chemical shifts for histidine (H44) protons are highlighted in (C) with the arrows.

reported. To confirm the basic features of the C-terminal finger-RNA(DNA) interaction, the binding to the hexanucleotide d(TACGCC) was studied. The sequence was chosen to compare with previous studies, and the extra thymine was added to contribute additional stability to the peptide-oligonucleotide complex, especially given the presence of a number of lysine residues in the peptide. Addition of d(TACGCG) to the peptide resulted in a progressive shift of the protein resonances, indicative of fast exchange. The resonances were assigned from 2D NOESY and COSY data sets. The full list of assigned chemical shifts is given in Table S1A. For the protein, three stretches of NH-NH connectivities are present: from Lys(5)-Glu(9), from Lys(14)-Cys(16), and from Thr(17)-Glu(18). The $d_{\alpha N}$ sequential assignment is present from Lys(5)-Glu(9) and from Met(13)-Glu(18). Comparison of the NOESY spectra in H_2O and D_2O allowed unambiguous assignment of the nonexchangeable aromatic H's of the His and Trp residues, and long-range NOEs between these two aromatic residues are observed. The aromatic proton resonances of the tryptophan residue all show an upfield shift during the titration ($\delta H^{\delta 1}$ 0.34 ppm, $\delta H^{\varepsilon 1}$ 0.33 ppm, $\delta H^{\zeta 2}$ 0.38 ppm, $\delta H^{\eta 2}$ 0.03 ppm, $\delta H^{\zeta 3}$ 1.20 ppm, and $\delta H^{\varepsilon 3}$ 0.64 ppm), indicating electrostatic interactions between the nucleobases and the tryptophan ring. Another indication for strong interactions between the oligonucleotide and the protein is the appearance of new NH resonances during the titration, which can be assigned to oligonucleotide NH's (see below) and the progressive sharpening of the original broad water signal upon addition of d(TACGCC). This reduced exchange broadening of NH with the solvent can be ascribed to protein-oligonucleotide interactions (i.e., shielding the exchangeable H's from the solvent and/or the presence of H-bonding interactions between the oligonucleotide and the protein).

The 2D NMR data gave a more detailed picture of the DNA-protein interactions. The full set of NOE restraints did not allow an unambiguous structure determination, but the main features of the interaction may be deduced. Figure 3A shows the region from a NOESY data set containing contacts between base protons from the DNA hexamer and aromatic protons from the F2 peptide. In this region, weak crosspeaks are observed between C_3H5 and both W4-Hζ3 and W4-Hε3, while stronger crosspeaks are observed between one of the exoyclic NH_2 protons of G_4 and W4-Hζ3. In Figure 3B, crosspeaks are noted between T_1H6 and K14-Hε2 and between A_2H2 and K14-Hγ1, which clearly indicate that the K14 side chain is also involved in intermolecular interactions. Note the presence of close contacts between the thymine and lysine residues seen from the NMR data. As a result of intermolecular interactions involving C_3 and G_4, the sequential assignment is interrupted between C_3 and G_4. These results are consistent with destacking of the cytosine from the nucleic acid single strand, as indicated by the break in connectivity between C_3 and G_4, rather than a formal intercalation of the tryptophan ring between the adjacent C_3 and G_4 bases. The structure of the complex formed between NCp10 from Moloney murine leukemia virus and the pentanucleotide d(ACGCC) studied by NMR methods showed insertion of Trp between two successive bases and its stacking to dG [35].

Zinc Finger Interaction with Platinated Nucleobases. NonCovalent Interactions

Once the essential nature of the F2-DNA interaction had been determined, we aimed to mimic this interaction with small molecules. Addition of the hexanucleotide to F2 caused the quenching of the tryptophan fluorescence to a large degree, in agreement with previous studies [36, 37]. Upon incubation of F2 with [Pt(dien)(9-EtGH)]$^{2+}$, **Ia**, the fluorescence intensity also decreased, and the fluorescence quenching is more effective than for free nucleobase, as observed previously. Similar enhancement is also found for platinated 5′-GMP, (**Ib**, [Pt(dien)(5′-GMP)]). The association constant values found by using Eadie-Hofstee analysis are 7.5×10^3, 12.4×10^3, and 60.0×10^3 M^{-1} for **Ia**, **Ib**, and d(TACGCC), respectively. Interestingly, while there is little difference in tryptophan binding between the 9-EtGH and 5′-GMP species, the extra phosphate group enhances binding to the zinc finger (Figure 4). The ribose monophosphate moiety could be involved in extra recognition features of the type Lys-phosphate previously reported for the complex NCp7/ACGCC [16]. While binding is predictably not as high as for free hexanucleotide, the results indicate that further incremental increases can be achieved by extending the length of the oligonucleotide chain bound to Pt.

The zinc finger-DNA interaction is amenable to study by mass spectrometry [38]. The ESI-MS spectrum of F2 in the presence of a 1:1 ratio of [Pt(dien)(9-EtGH)]$^{2+}$

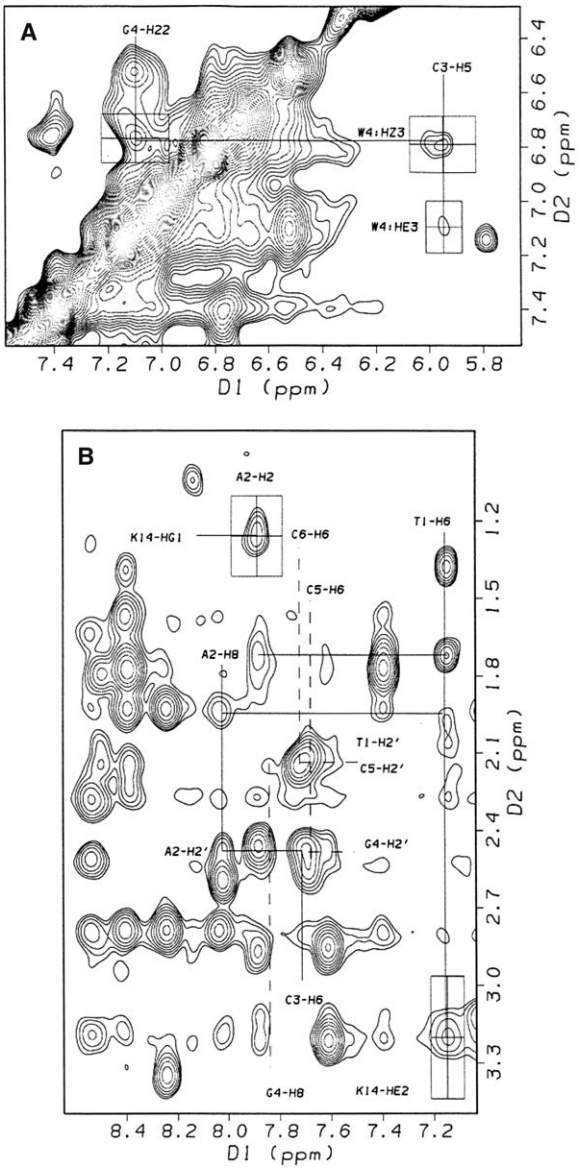

Figure 3. F2-Oligonucleotide Interaction

Expanded regions from a 200 ms NOESY data set obtained on d(TACGCC)-NCp7-F2(Zn) (in H_2O,D_2O [90:10], 298K) showing: (A) intermolecular NOE contacts between the aromatic protons of the TRP residue and C_3H5 and G_4NH22 of the oligonucleotide. (B) H_{base}-H2′/H2″ connectivities of d(TACGCC). Note the sequential "break" between C_3 and G_4, caused by the interaction with the Trp residue. Sequential H6/H8,H2′/H2″ connectivities are observed for T_1, G_2, and C_3; however, no connectivities are observed from either C_3H2' or C_3H2'' to G_4H8. The sequential walk resumes for C_5 as H2′/H2″; H6 connectivities are observed for C_5 and C_6. In addition, intermolecular connectivities between protons on the K14 side chain and T_1 and A_2 are shown.

shows a new peak at m/z = 923.47, corresponding to the 3+ state of the 1:1 adduct between the peptide and Pt complex (Figure 5A). MS-MS experiments on the peak at m/z = 923.47 shows dissociation to reactants and a minor peak at m/z = 1293.93, corresponding to the 2+ state of a F2/[Pt(dien)] adduct implying loss of 9-EtGH (Figure 5B).

Interestingly, the ESI-MS of F2 in the presence of free 9-Ethylguanine itself shows the presence of multiple

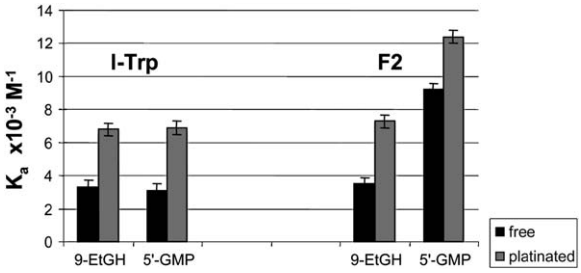

Figure 4. Noncovalent Interaction of Platinum Complexes—Fluorescence

Comparison between association constants determined for Pt-nucleobase/nucleotide complexes with N-acetyl tryptophan (left) and F2 (right). Bars represent the mean ± 0.3 × 10^{-3} M^{-1}.

adducts with more than one purine associated with the peptide (Figure S1A). The predominant adducts are the 1:1 (m/z = 1234.47) and 2:1 (m/z = 1324.40), but higher stoichiometries of 3:1 are also observed. Since only one aromatic residue (W37) is available for stacking, the presence of 1:2 and higher ratio adducts suggests additional extra noncovalent cation-π interactions given the positively charged lysines (4) and arginine (1) residues present in F2 [39]. In this regard, cation-π interactions have been found to occur with a higher frequency than π-π stacking interactions in protein/nucleic acid base systems [40]. Coordinate bond formation between the Zn and 9-EtGH forming a five-coordinate complex is also possible since the F2/9-EtGH specie was observed when *trans*-$[PtCl(py)_2(9\text{-EtGH})]^+$ was used (see below). The observation of multiple adducts may be due to the gas phase nature of the reactions—in solution, the platinated 9-Ethylguanine interacts more strongly than the free base with both simple tryptophan and F2 (Figure 4).

In the case of the F2/5′-GMP system only the 1:1 adduct was observed (Figure S1B). The presence of 1:1 adducts between N-AcTrp, as a model of W37 in F2, and the complex [Pt(dien)(5′-GMP)] have also been detected via ESI-MS (Figure S2), but mass spectra with the hexanucleotide d(TACGCC) were very noisy and were not pursued at this time.

The CD spectrum of F2 in presence of $[Pt(dien)(9\text{-EtGH})]^{2+}$ shows little perturbation of the secondary metallopeptide structure (data not shown). A reasonable interpretation of the results then is that adduct formation has occurred between the F2 and $[Pt(dien)(9\text{-EtGH})]^+$ facilitated by the π-π stacking between tryptophan and the platinated purine nucleobase, but this association does not disrupt the three-dimensional structure of F2 to a significant degree. Covalent interaction on the other hand proves to have significantly different consequences (vide infra).

The incubation of *cis*-$[Pt(NH_3)_2(Guo)_2]^{2+}$ (Guo, guanosine; **III**) with F2 showed a very small peak at m/z = 1029.40 amu corresponding to association to the 1:1 adduct $[Pt(NH_3)(Guo)_2/F2]^{3+}$. The peak assignment was supported by comparison of the calculated isotopic distribution. An MS2 experiment on the peak clearly revealed signals assignable to the free F2 and the platinum complex, indicating dissociation (Figure S3). The presence of these species again implies a chemical model for DNA recognition. The binding is much weaker than

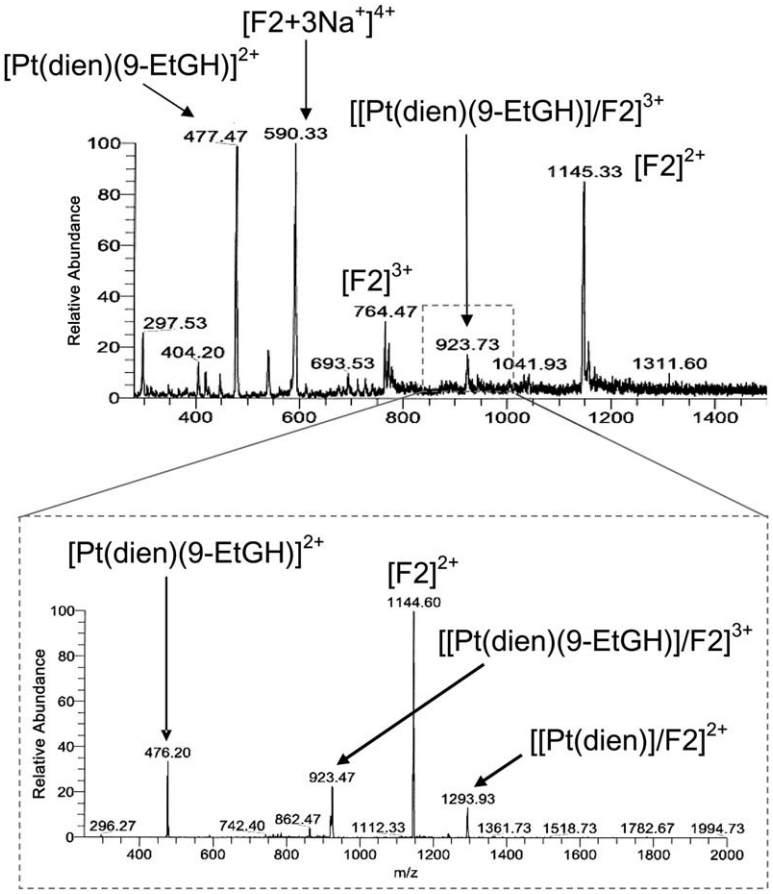

Figure 5. Noncovalent Interaction of Platinum Complexes—ESI-MS

Full ESI-MS spectrum of the 1:1 incubation for [Pt(dien)(9-EtGH)] with F2 (A), MS2 from the species at 923.73 m/z, confirming the assignation of the signal to the 1:1 adduct $[[Pt(dien)(9\text{-EtGH})]/F2]^{3+}$.

that of $[Pt(dien)(9\text{-EtGH})]^{2+}$, and thus there are distinctions between platinum complex structures in their interactions with zinc fingers. In this case, steric hinderance of the two *cis*-oriented purine nucleosides may account for the weaker binding. Studies of this compound are also of interest because of its previously reported antiviral activity [41, 42].

Zinc Finger Interaction with Platinated Nucleobases: Covalent Interaction and Zinc Ejection

To examine the possible covalent attachment of Pt to the Zn finger, the interaction was studied with *trans*-$[PtCl(9\text{-EtGH})(py)_2]^+$, **II**. This complex has previously been shown to have a high kinetic preference for sulfur (methionine) over nitrogen (5′-GMP) binding [43]. Further, Zn was shown to be ejected from model chelates in the presence of the complex [26]. In the presence of a 1:1 stoichiometric ratio of **II**, the ESI-MS spectrum of F2 after 24 hr now shows a number of peaks (Figure 6). Free 9-EtGH is observed and, again, a 1:1 adduct of F2 and 9-EtGH is seen with a peak at 1233.5 (2+ state). Interestingly a peak corresponding to *trans*-$[Pt(py)_2(9\text{-EtGH})_2]^{2+}$ is also seen at m/z of 355.7. A reasonable interpretation of these results is that formation of a Zn-S-Pt intermediate will labilize the *trans* 9-EtGH ligand due to the strong *trans* influence of thiolate. Free 9-EtGH may then form the five-coordinate species with Zn and substitute Cl in **II**. The species of interest in the mass spectrum is firstly that assigned to F2 + $[Pt(py)_2]$: m/z = 1320.1 (2+), 880.5 (+3), and 655.3 (+4). The isotopic distribution is consistent with a Pt, Zn species (data not shown). As observed previously, the presence of multiple isotopes in transition metals makes analysis of isotopic distribution a very useful asset in assigning stoichiometry [26]. The second major species of interest is that with m/z values for a 2+, 3+, and 4+ state of 1464.1, 976.5, and 733.3, respectively. This species corresponds to an adduct $([F2(Pt[py]_2)_2]\text{-Zn})$. That is, two $[Pt(py)]_2$ units are bound to the protein with resultant loss of the zinc atom. The isotopic distribution of this peak is also consistent with only two Pt atoms and no Zn. Tandem MS/MS of the 733.3 (4+) state showed sequential loss of four pyridine ligands leading to the observation of 4+ state fragments with m/z of 712.5, 693.0, 673.2, and 653.5. The corresponding 3+ state peaks at m/z of 949.7, 923.4, 897.0, and 870.6 were observed as well, and the isotopic distribution of the latter peak (m/z of 870.6) was also consistent with the presence of two Pt atoms (Figure 6B). Essentially identical behavior was observed with *[SP-4-2]*-$[PtCl(9\text{-EtGH})(NH_3)(quin)]^+$ (data not shown) indicating that this chemistry is a general feature of this class of compounds. After 7 days incubation, the major species observed were *trans*-$[Pt(py)_2(9\text{-EtGH})_2]^{2+}$ (m/z = 355.7), $(F2 + [Pt(py_2)]_2)^{3+}$ (m/z = 880.5), $(F2 + 2[Pt(py)_2] - Zn)^{3+}$ (m/z = 976.5), and $(F2 + 9\text{-EtGH})^{2+}$ (m/z = 1233.5) (see Figure S4).

The CD spectra of F2 in presence of *trans*-$[PtCl(9\text{-EtGH})(py)_2]^+$ is shown in Figure 6C. Monitoring of the spectrum through time revealed important changes in the three-dimensional structure of F2 within the first

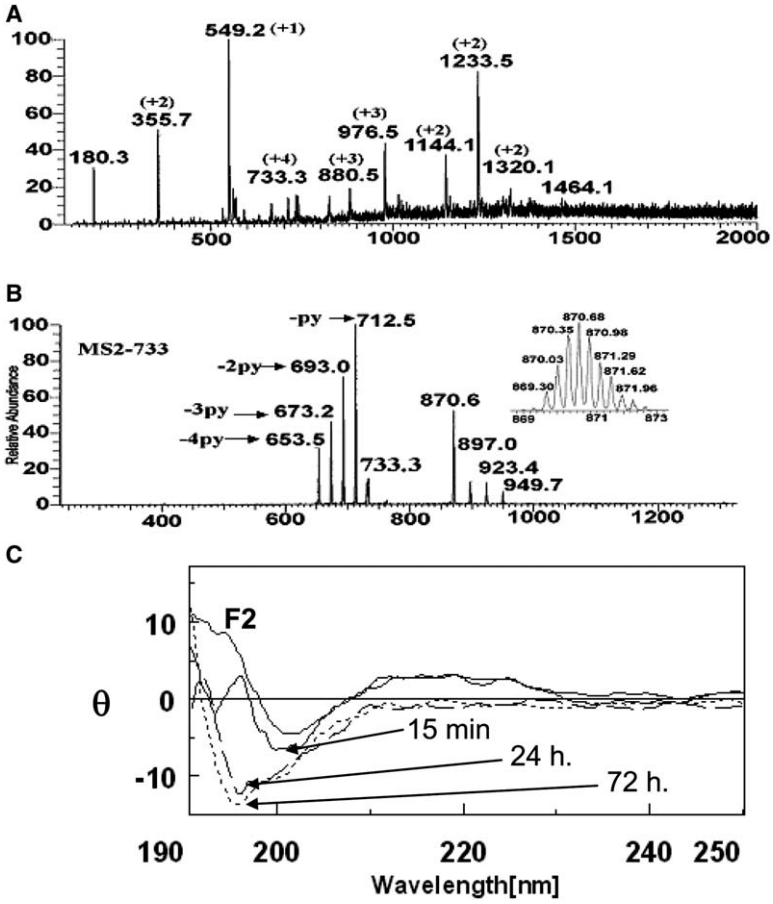

Figure 6. Covalent Interaction F2/Platinum Complex

Covalent interaction between F2 and *trans*-$[PtCl(py)_2(9\text{-EtGH})]^+$: (A) ESI-MS spectrum after 24 hr; incubation shows 1:1 adducts of the platinum complex and F2 (m/z = 1320.1, 880.5, and 655.3), also signals corresponding to two $Pt(py)_2$ units with the free peptide (m/z = 1464.1, 976.5, and 733.3), indicating loss of the zinc ion; (B) tandem MS/MS experiments and isotopic distribution of the signals confirmed the assignation; (C) CD spectra of F2 undergo a blueshift of the ellipticity minimum after incubation with 2 eq. *trans*-$[PtCl(py)_2(9\text{-EtGH})]^+$; after 72 hr, the spectrum is very similar to the free peptide. Intact F2 is shown as a reference.

24 hr. It is clear that the loss of structural feature is consistent with loss of tertiary structure due to Zn elimination.

Discussion

The results presented here suggest that modulation of the basic $[PtCl(L)(L')(Nucleobase)]^+$ (L = NH_3, L′ = py, quin, etc., or L = L′ = py, etc.) structural motif is a viable approach to more effective and selective inhibitors of the zinc-finger-nucleic acid interaction. The concept mechanism involving a classic two-step approach: (1) target recognition through tryptophan interaction and (2) target fixation or inhibition involving platinum-protein complexation followed by zinc ejection is shown in Figure 7A. The proposed chemical mechanism shown in Figure 7B is reasonable based on previous results with zinc fingers and with model zinc chelates [26, 28, 46]. Subsequent reactions including incorporation of platinum into the finger are possible.

The results are of interest for two main reasons. First, study of metal displacement of zinc from zinc-finger or zinc-based proteins has probed the potential biomedical implications involved in incorporation of metals such as Cd, Hg, Pb, and Ni (usually studied as aquated 2+ cations) [30, 44]. The reactions of gold thiomalate with the Sp1 zinc finger [31] and the use of oligonucleotide-tethered cobalt (salen) as a sequence-specific recognition probe [45] are, in principle, examples of zinc finger interaction with *functionalized* metal complexes. The results presented here indicate that functionalized platinum complexes (in this case the presence of purine nucleobases and the absence or presence of substitution-labile binding site) display a variety of chemical reactivity on the Zn-finger site. While the present study demonstrates the use of Cys_3His finger, it would be expected that the different limiting Zn-finger coordination sites would also display different chemical reactivity [28] In this context, the reaction between cisplatin and a 31-amino acid zinc finger sequence (zpp) N-I **C_1** E E P T **C_1** R N R T R H L P L Q F S R T G P L **C_2** P A **C_2** M K A is noteworthy [46]. The reaction proceeds in a stepwise manner, and complete deligation of Zn(II) was only observed with two equivalent of *cis*-DDP [46]. The subscripted residues represent the four Zn ligands and the sites of the first and second attachment of platinum, respectively. These results have been discussed with respect to apoptosis initiated by direct interaction of the platinum antitumor agent with zinc finger transcription factors, but it is of interest to note that two Pt atoms appear necessary before zinc is lost from the peptide. In the case of F2, the possible sulfur binding sites on F2 include the methionine and the three Zn bound cysteines. It is possible that the first platination occurs at the methionine site, and this may not disturb the zinc coordination sphere. The second platination would then involve a ligand intimately involved in maintaining the tetrahedral zinc geometry, and loss of Zn could then occur, as seen in model systems. Evidence for competitive binding of methionine in proteins rather than cysteine has come from studies of cisplatin with human serum albumin [47]. The use of *trans*-DDP

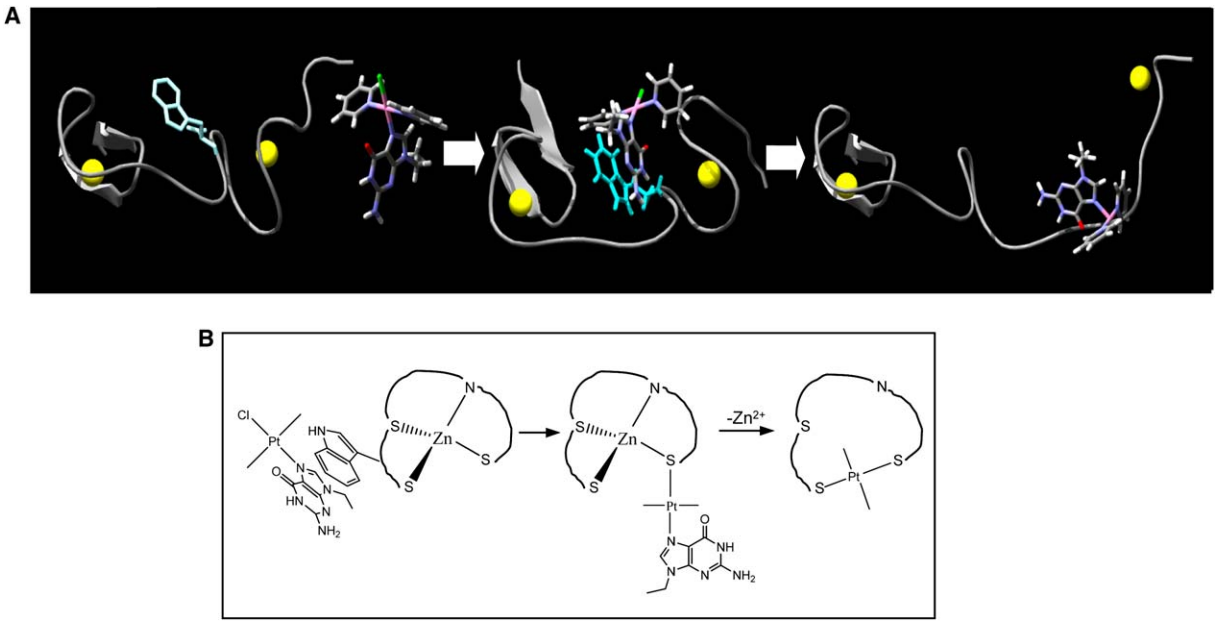

Figure 7. Schematic Mechanism of Action

(A) Proposed concept mechanism of zinc ejection from F2 involving an initial recognition process through noncovalent interactions and a further covalent interaction that eventually disrupts the secondary structure in the protein.

(B) A chemical mechanism for zinc ejection using platinum-nucleobase electrophiles. The specific nature of the coordination site for the $[Pt(py)_2]$ unit remains to be determined.

to crosslink the zinc finger nucleocapsid protein to HIV-1 RNA has been reported [10], and the specific interactions are likely to be similar to those described here.

Secondly, these results suggest novel approaches to targeting the nucleic acid-zinc finger interaction. Most approaches to NCp7 inhibition have involved alkylation or oxidation of the cysteine residues, resulting in reduced ability to bind zinc and subsequent loss of conformation thereby diminishing or eliminating infectivity [20]. The small organic molecules designed for electrophilic attack have little or no DNA selectivity, therefore precluding attack on the protein-DNA interaction. The presence of an aromatic residue—tryptophan, phenylalanine, and tyrosine—as a recognition motif for single-stranded DNA and RNA is a structural handle one can use in inhibitor design. A study of oligonucleotide affinity for HIV nucleocapsid protein showed that small GT sequences such as $d(GT)_4$ had high binding affinity, and indeed this property has been used as a screen for nucleic acid antagonists of NCp7 [48]. The incipient and moderately selective *antiviral* activity of *trans*-$[PtCl(Nucleobase)(L)(L')]^+$ is worthy of further rational study based on the concept hypothesis [49].

Significance

This contribution shows that the interaction of small molecules such as *trans*-$[PtCl(9\text{-EtGH})(py)_2]^+$ with the C-terminal zinc finger of HIV-NCp7 protein results in Zn ejection from the peptide accompanied by loss of tertiary structure. The nature of the protein-DNA interaction on the C-terminal finger alone with the hexanucleotide d(TACGCT) was examined. The results confirm the tryptophan-guanine/cytosine recognition motif for zinc finger-single-stranded DNA/RNA interactions and may be placed in context with structural examinations of the N-terminal finger and the intact 2-zinc finger peptide with similar DNA sequences. The platinated nucleobase motif of complexes I and II mimics the DNA-protein stacking interaction. Targeting the NCp7-DNA interaction for drug design represents a conceptual advance over electrophiles designed for chemical attack on the zinc finger alone. Thus, complex II is a first example of a new chemotype capable of *selective* zinc finger attack through targeting of the tryptophan/guanine recognition. In a broader sense, these results demonstrate examples of a new platinum structural class targeting specific biological processes, distinct from the bifunctional DNA-DNA binding of cytotoxic agents like cisplatin. Extension of this analogy between Me^+ and Pt^{2+} can suggest further novel structural motifs capable of expanding the role of platinum in biology beyond the current paradigm. An important goal for medicinal inorganic chemists is to manipulate the many intrinsic features of transition metal complexes—the number and type of exchangeable ligands, oxidation state of the central metal ion, coordination number, and stereochemistry as well as rate of reaction—to design more selective agents capable of targeting specific biomolecules and thus eventually capable of exerting a more specific biological response.

Experimental Procedures

Starting Materials. Preparation of F2

Coordination of the zinc ion to the peptide (34–52) and secondary structure characterization of the F2 zinc finger were monitored by

^{1}H-NMR, ESI-MS, and CD spectroscopy, and the data obtained were in agreement with reported values in the literature [30, 45].

The C-terminal zinc finger from the retroviral HIV-1 p7 nucleocapsid protein (F2, sequence Lys-Gly-Cys-Trp-Lys-Cys-Gly-Lys-Glu-Gly-His-Gln-Met-Lys-Asp-Cys-Thr-Glu) was purchased from the Macromolecular Structure Facility of the University of Arizona (Division of Biotechnology). The peptide was dissolved in degassed H_2O solution (HPLC-grade, J.T. Baker) and $ZnCl_2$ (1.2 equimolar) was added in slight excess with respect to the concentration of the zinc finger. The pH was adjusted to 6.4, and the sample was lyophilized. The oligonucleotide d(TACGCC) was synthesized with an Expedite 8909 DNA synthesizer (Perseptive Biosystems) by the cyanoethyl phosphoramidite method (reagents were from Glen Research, Sterling, VA).

NMR Spectroscopy

All NMR spectra were acquired at 298 K and pH 6.4 on a Varian Unity 500 MHZ spectrometer at 2.9 mM concentration. ^{1}H NMR chemical shifts were referenced to internal H_2O (4.72 ppm at 298 K) and ^{31}P NMR data are referenced to trimethyl phosphate (TMP). 2D NMR data were collected without sample spinning. 2D NOESY data were recorded in 90% H_2O/10% D_2O (t_{mix} 100, 200, and 400 ms) and in D_2O (99.99%, t_{mix} 300 ms). The nonexchangeable NOESY spectrum was recorded by the States/TPPI technique with 512 t_1 increments and a sweep width of 6802.72 Hz. Solvent suppression for the homonuclear 2D measurements in H_2O was achieved by the watergate technique. 512 t_1 increments, each with 1024 t_2 complex points, were collected with a SW of 6802.72 Hz. For the TOCSY experiment, a t_{mix} of 80 ms was used. The 2QF-COSY was measured according to literature procedures [50]. The 2D heteronuclear ^{31}P-^{1}H correlation spectra were recorded by the method described [51]. The data were processed by using the Felix 2.10 software (BioSym Technologies) with a cosine-bell function before Fourier transformation.

Assignment of Protein and Oligonucleotide Resonances

The protein resonances of the d(TACGCC)-HIVF2 complex were assigned according to established procedures [52]. A summary of the protein assignments is listed in Table S1A. Interesidual NOEs between the four residues coordinated to the zinc confirm their spatial proximity. The NH^{ε} protons of Gln(12) can be observed in the TOCSY from a long-range coupling toward the H^{γ}(12). The chemical shifts of the oligonucleotide moiety are summarized in Table S1B.

Electrospray Ionization Mass Spectrometry Method

Electrospray ionization mass spectra (ESI-MS) were recorded by Finnigan LCQ ion-trap electrospray meter (LCQ-MS) in positive mode. The employed voltage at the electrospray needles was 2.5 kV. The capillary was heated to 150ºC. The solutions were injected into the Nano-ESI source directly at the flow rate of 1.0 μl/min. Tandem mass and zoom scan were used to analyze the structure of the product. Helium gas was admitted directly into the ion trapping efficiency and as collision gas in the collision-induced dissociation (CID) experiment. A maximum ion injection time of 500 ms along with ten scans was set. To induce collision activation, the relative collision energy was controlled to 10%–30% of maximum, depending on the precursor ions and the MS^n. In MS/MS experiments, 6–12 isolation width for the precursor ions were used to allow the Pt isotopic signature to be observed.

Circular Dichroism Spectropolarimetry

The circular dichroism (CD) spectra were recorded in a JASCO J-600 Spectropolarimeter (Jasco, Corp., Tokyo, Japan). The pH of the solutions was maintained in the range 6.9–7.4 by addition of NaOH solution. Each spectrum was recorded at a wavelength range 190–250 nm in a 0.1 cm cuvette path length at room temperature under N_2. Spectra were baseline-corrected and noise-reduced with the Jasco software.

Fluorescence Spectrophotometry

The fluorescence spectra were recorded in a Varian Cary Eclipse fluorescence spectrophotometer equipped with a single-cell Peltier accessory. Fluorescence spectra were recorded in the range of 295 to 450 nm with a scan rate of 120 nm/min. The maximum intensity of the spectrum (at ca 362.9 and 358.9 nm for N-AcTrp and F2, respectively) was measured for each addition, and the association constants for each system were obtained from the analysis of Eadie-Hofstee plots [53]. Measurements were made at 20ºC, and reported association constants (K_a) were averaged over a number of six different experiments, with the significance of results compared by using the unpaired t test.

Supplemental Data

Supplemental data include tables of ^{1}H NMR chemical shift assignments for the protein (Table S1A) and oligonucleotide (Table S1B) moieties of d(TACGCC)-NCp7, ESI-MS spectra of 9-EtGH, 5′-GMP and *trans*-$[PtCl(9\text{-}EtGH)(py)_2]^+$ with F2, N-AcTrp with Pt(dien)5′-GMP, and tandem MS for *cis*-$[Pt(NH_3)_2(Guo)_2]$/F2 and may be found at http://www.chembiol.com/cgi/content/full/13/5/539/DC1/.

Acknowledgments

This research was supported by The National Science Foundation and The American Cancer Society. A.I.A. contributed the spectroscopic data for this paper, M.J.B. contributed the NMR data, and Q.L. to the mass spectrometric data.

Received: February 20, 2006
Revised: March 30, 2006
Accepted: April 3, 2006
Published: May 29, 2006

References

1. Summers, M.F., Henderson, L.E., Chance, M.R., Bess, J.W., South, T.L., Blake, P.R., Sagi, I., Perez-Alvarado, G., Sowder, R.C., Hare, D.R., et al. (1992). Nucleocapsid zinc fingers detected in retroviruses: EXAFS studies of intact viruses and the solution-state structure of the nucleocapsid protein from HIV-1. Protein Sci. *1*, 563–574.
2. Bess, J.W., Jr., Powell, P.J., Issaq, H.J., Schumack, L.J., Grimes, M.K., Henderson, L.E., and Arthur, L.O. (1992). Tightly bound zinc in human immunodeficiency virus type *1*, human T-cell leukemia virus type I, and other retroviruses. J. Virol. *66*, 840–847.
3. Gorelick, R.J., Nigida, S.M., Jr., Bess, J.W., Jr., Aurthor, L.O., Henderson, L.E., and Rein, A. (1990). Noninfectious human immunodeficiency virus type 1 mutants deficient in genomic RNA. J. Virol. *64*, 3207–3211.
4. Mely, Y., de Rocquigny, H., Sorinas-Jimeno, M., Keith, G., Roques, B.P., Marquet, R., and Gerard, D. (1995). Binding of the HIV-1 nucleocapsid protein to the primer tRNA3Lys, in vitro, is essentially not specific. J. Biol. Chem. *270*, 1650–1656.
5. Khan, R., and Giedroc, D.P. (1994). Nucleic acid binding properties of recombinant Zn2 HIV-1 nucleocapsid protein are modulated by COOH-terminal processing. J. Biol. Chem. *269*, 22538–22546.
6. Surovoy, A., Dannull, J., Moelling, K., and Jung, G. (1993). Conformational and nucleic acid binding studies on the synthetic nucleocapsid protein of HIV-1. J. Mol. Biol. *229*, 94–104.
7. Herschlag, D.J. (1995). RNA chaperones and the RNA folding problem. J. Biol. Chem. *270*, 20871–20873.
8. Gorelick, R.J., Nigida, S.M., Jr., Bess, J.W., Jr., Arthur, L.O., Henderson, L.E., and Rein, A. (1990). Noninfectious human immunodeficiency virus type 1 mutants deficient in genomic RNA. J. Virol. *64*, 3207–3211.
9. Sakaguchi, K., Zambrano, N., Baldwin, E.T., Shapiro, B.A., Erickson, J.W., Omichinski, J.G., Clore, G.M., Gronenborn, A.M., and Appella, E. (1993). Identification of a binding site for the human immunodeficiency virus type 1 nucleocapsid protein. Proc. Natl. Acad. Sci. USA *90*, 5219–5223.
10. Darlix, J.L., Gabus, C., Nugeyre, M.T., Clavel, F., and Barre-Sinoussi, F. (1990). Cis elements and trans-acting factors involved in the RNA dimerization of the human immunodeficiency virus HIV-1. J. Mol. Biol. *216*, 689–699.
11. Barat, C., Lullien, V., Schatz, O., Keith, G., Nugeyre, M.T., Gruninger-Leitch, F., Barre-Sinoussi, F., LeGrice, S.F., and Darlix, J.L. (1989). HIV-1 reverse transcriptase specifically interacts with the anticodon domain of its cognate primer tRNA. EMBO J. *8*, 3279–3285.

12. Barat, C., Le Grice, S.F., and Darlix, J.L. (1991). Interaction of HIV-1 reverse transcriptase with a synthetic form of its replication primer, tRNA(Lys,3). Nucleic Acids Res. *19*, 751–757.
13. Venter, J.C., Adams, M.D., Myers, E.W., Li, P.W., Mural, R.J., Sutton, G.G., Smith, H.O., Yandell, M., Evans, C.A., Holt, R.A., et al. (2001). The sequence of the human genome. Science *291*, 1304–1313.
14. Hoovers, J.M.N., Mannens, M., John, R., Bliek, J., van Heyningen, V., Porteous, D.J., Leschot, N.J., Westerveld, A., and Little, P.F.R. (1992). High-resolution localization of 69 potential human zinc finger protein genes: a number are clustered. Genomics *12*, 254–263.
15. De Guzman, R.N., Wu, Z.R., Stalling, C.C., Pappalardo, L., Borer, P.N., and Summers, M.F. (1998). Structure of the HIV-1 nucleocapsid protein bound to the SL3 Ψ-RNA recognition element. Science *279*, 384–388.
16. Morellet, N., Déméné, H., Teilleux, V., Huynh-Dinh, T., de Rocquigny, H., Fournié-Zaluski, M.C., and Roques, B.P. (1998). Structure of the complex between the HIV-1 nucleocapsid protein NCp7 and the single-stranded pentanucleotide d(ACGCC). J. Mol. Biol. *283*, 419–434.
17. de Rocquigny, H., Delaunay, T., Petitjean, P., Fournié-Zaluski, M.C., and Roques, B.P. (1998). La structure native de la NCp7 d'HIV-1 est nécessaire pour la reconnaissance spécifique de la séquence d'encapsidation psi de l'ARN genomique: etude par résonance plasmonique de surface. Reg. Biochimie *2*, 44–50.
18. Remy, E., de Rocquigny, H., Petitjean, P., Muriaux, D., Theilleux, V., Paoletti, J., and Roques, B.P. (1998). The annealing of tRNA3Lys to human immunodeficiency virus type 1 primer binding site is critically dependent on the NCp7 zinc fingers structure. J. Biol. Chem. *273*, 4819–4822.
19. Amarasinghe, G.K., de Guzman, R.N., Turner, R.B., Chancellor, K.J., Wu, Z.R., and Summers, M.F. (2000). NMR structure of the HIV-1 nucleocapsid protein bound to stem-loop SL2 of the Ψ-RNA packaging signal. Implications for genome recognition. J. Mol. Biol. *301*, 491–511.
20. Musah, R.A. (2004). The HIV-1 nucleocapsid zinc finger protein as a target of antiretroviral therapy. Curr. Top. Med. Chem. *4*, 1605–1622.
21. Stephen, A.G., Worthy, K.M., Towler, E., Mikovits, J.A., Sei, S., Roberts, P., Yang, Q.E., Akee, R.K., Klausmeyer, P., McCloud, T.G., et al. (2002). Identification of HIV-1 nucleocapsid protein:nucleic acid antagonists with cellular anti-HIV activity. Biochem. Biophys. Res. Commun. *296*, 1228–1237.
22. Huang, M., Maynard, A., Turpin, J.A., Graham, L., Janini, G.M., Covell, D.G., and Rice, W.G. (1998). Anti-HIV agents that selectively target retroviral nucleocapsid protein zinc fingers without affecting cellular zinc finger proteins. J. Med. Chem. *41*, 1371–1381.
23. Anzellotti, A.I., Ma, E.S., and Farrell, N. (2005). Platination of nucleobases to enhance non-covalent recognition in protein-DNA/RNA complexes. Inorg. Chem. *44*, 483–485.
24. Anzellotti, A.I., Sabat, M., and Farrell, N. (2006). Covalent and noncovalent interactions for $[Metal(dien)nucleobase]^{2+}$ complexes with l-tryptophan derivatives: formation of palladium-tryptophan species by nucleobase substitution under biologically relevant conditions. Inorg. Chem. *45*, 1638–1645.
25. Ishida, T., Ueda, H., Segawa, K., Doi, M., and Inoue, M. (1990). Prominent stacking interaction with aromatic amino acid by N-quarternization of nucleic acid base: X-ray crystallographic characteristics and biological implications. Arch. Biochem. Biophys. *278*, 217–227.
26. Liu, Q., Golden, M., Darensbourg, M.Y., and Farrell, N. (2005). Thiolate-bridged heterodinuclear platinum-zinc chelates as models for ternary platinum-DNA-protein complexes and zinc ejection from zinc fingers. Evidence from studies using ESI-mass spectrometry. Chem. Commun. *34*, 4360–4362.
27. Wilker, J.J., and Lippard, S.J. (1997). Alkyl transfer to metal thiolates: kinetics, active species identification, and relevance to the DNA methyl phosphotriester repair center of *Escherichia coli* ADA. Inorg. Chem. *36*, 969–978.
28. Maynard, A.T., and Covell, D.G. (2001). Reactivity of zinc finger cores: analysis of protein packing and electrostatic screening. J. Am. Chem. Soc. *123*, 1047–1058.
29. Nomura, A., and Sugiura, Y. (2002). Contribution of individual zinc ligands to metal binding and peptide folding of zinc finger peptides. Inorg. Chem. *41*, 3693–3698.
30. Kopera, E., Schwerdtle, T., Hartwig, A., and Bal, W. (2004). Co(II) and Cd(II) substitute for Zn(II) in the zinc finger derived from the DNA repair protein XPA, demonstrating a variety of potential mechanisms of toxicity. Chem. Res. Toxicol. *17*, 1452–1458.
31. Larabee, J.L., Hocker, J.R., and Hanas, J.S. (2005). Mechanisms of aurothiomalate-Cys2His2 zinc finger interactions. Chem. Res. Toxicol. *18*, 1943–1954.
32. South, T.L., Blake, P.R., Hare, D.R., and Summers, M.F. (1991). C-terminal retroviral-type zinc finger domain from the HIV-1 nucleocapsid protein is structurally similar to the N-terminal zinc finger domain. Biochemistry *30*, 6342–6349.
33. Delahunty, M.D., South, T.L., Summers, M.F., and Karpel, R.L. (1992). Nucleic acid interactive properties of a peptide corresponding to the N-terminal zinc finger domain of HIV-1 nucleocapsid protein. Biochemistry *31*, 6461–6469.
34. Summers, M.F., Henderson, L.E., Chance, M.R., Bess, J.W., Jr., South, T.L., Blake, P.R., Sagi, I., Perez-Alvarado, G., Sowder, R.C., III, Hare, D.R., et al. (1992). Nucleocapsid zinc fingers detected in retroviruses: EXAFS studies of intact viruses and the solution-state structure of the nucleocapsid protein from HIV-1. Protein Sci. *1*, 563–574.
35. Schuler, W., Dong, C.-Z., Wecker, K., and Roques, B.P. (1999). NMR Structure of the complex between the zinc finger protein NCp10 of Moloney murine leukemia virus and the single-stranded pentanucleotide d(ACGCC): comparison with HIV-NCp7 complexes. Biochemistry *38*, 12984–12994.
36. Vuilleumier, C., Bombarda, E., Morellet, N., Gerard, D., and Roques, B.P. (1999). Nucleic acid sequence discrimination by the HIV-1 nucleocapside proetin NCp7: a fluorescence study. Biochemistry *38*, 16816–16825.
37. Bombarda, E., Ababou, A., Vuilleumier, C., Gérard, D., Roques, B.P., Piémont, E., and Mély, Y. (1999). Time-resolved fluorescence investigation of the human immunodeficiency virus type 1 nucleocapsid protein: influence of the binding of nucleic acids. Biophys. J. *76*, 1561–1570.
38. Loo, J.A. (1997). Studying noncovalent protein complexes by electrospray ionization mass spectrometry. Mass Spectrom. Rev. *16*, 1–23.
39. Ma, J.C., and Dougherty, D.A. (1997). The cation-π interaction. Chem. Rev. *97*, 1303–1324.
40. Biot, C., Buisine, E., Kwasigroch, J.M., Wintjens, R., and Rooman, M. (2002). Probing the energetic and structural role of amino acid/nucleobase cation-pi interactions in protein-ligand complexes. J. Biol. Chem. *277*, 40816–40822.
41. Snyder, M.B., Saravolatz, L.D., Markowitz, N., Pohlod, D., Taylor, R.C., and Ward, S. (1987). The in-vitro and in-vivo efficacy of cisplatin and analogues in the treatment of herpes simplex virus-II infections. J. Antimicrob. Chemother. *19*, 815–822.
42. Pommier, Y., Johnson, A.A., and Marchand, C. (2005). Integrase inhibitors to treat HIV/AIDS. Nat. Rev. Drug Discov. *4*, 236–248.
43. Anzellotti, A., Stefan, S., Gibson, D., and Farrell, N. (2006). Donor atom preferences in substitution reactions of *trans*-platinum mononucleobase compounds. Implications for DNA-protein selectivity. Inorg. Chim. Acta, in press.
44. Godwin, H.A., Payne, J.C., and ter Horst, M.A. (1999). Lead fingers: Pb^{2+} binding to structural zinc-binding domains determined directly by monitoring lead-thiolate charge-transfer bands. J. Am. Chem. Soc. *121*, 6850–6855.
45. Louie, A.Y., and Meade, T.J. (1998). A cobalt complex that selectively disrupts the structure and function of zinc fingers. Proc. Natl. Acad. Sci. USA *95*, 6663–6668.
46. Bose, R.N., Wei, W., Yang, W., and Evanics, F. (2005). Structural perturbation of a C4 zinc-finger module by cis-diamminedichloroplatinum(II): insights into the inhibition of transcription processes by the antitumor drug. Inorg. Chim. Acta *358*, 2844–2854.
47. Ivanov, A.I., Christodoulou, J., Parkinson, J.A., Barnham, K.J., Tucker, A., Woodrow, J., and Sadler, P.J. (1998). Cisplatin binding sites on human albumin. J. Biol. Chem. *273*, 14721–14730.
48. Stephen, A.G., Worthy, K.M., Towler, E., Mikovits, J.A., Sei, S., Roberts, P., Yang, Q., Akee, R.K., Klausmeyer, P., McCloud, T.G., et al. (2002). Identification of HIV-1 nucleocapsid protein:

nucleic acid antagonists with cellular anti-HIV activity. Biochem. Biophys. Res. Commun. *296*, 1228–1237.

49. Sartori, D.A., Miller, B., Bierbach, U., and Farrell, N. (2000). Modulation of the chemical and biological properties of trans platinum complexes: monofunctional platinum complexes containing one nucleobase as potential antiviral chemotypes. J. Biol. Inorg. Chem. *5*, 575–583.
50. Rance, M., Sorenson, O.W., Bodenhausen, G., Wagner, G., Ernst, R.R., and Wuthrich, K. (1983). Improved spectral resolution in cosy 1H NMR spectra of proteins via double quantum filtering. Biochem. Biophys. Res. Commun. *117*, 479–485.
51. Keniry, M.A. (1996). Pulsed field gradient pulse sequence for heteronuclear [31P-1H] long range correlation. Magn. Reson. Chem. *34*, 33–35.
52. Wütrich, K. (1986). NMR of Proteins and Nucleic Acids (New York: John Wiley & Sons).
53. Eadie, G.S. (1942). The inhibition of cholinesterase by physostigmine and prostigmine. J. Biol. Chem. *146*, 85–93.